Collapse of Landau levels in semi-Dirac materials

Daniil Asafov [1] and Ilia Pavlov [2]
[1] *California Institute of Technology, Pasadena, California 91125, USA*
[2] *School of Physics and Engineering, ITMO University, 197101 St. Petersburg, Russia*

(Received 20 February 2024; revised 23 July 2024; accepted 30 August 2024; published 11 September 2024)

Two-dimensional semi-Dirac models describe a family of novel materials that have anisotropic dispersion with a relativistic-type spectrum along one of the spatial directions and nonrelativistic along another. In the present paper we perform a detailed analysis of the collapse of Landau levels for such models in a perpendicular magnetic field and in-plane electric field by using a semiclassical approach. The anisotropic nature of semi-Dirac dispersion manifests itself in the possibility of a Landau level collapse for only one of the electric field directions. In addition, the topological transition with merging Dirac cones has its own distinct features in a Landau level collapse.

DOI: 10.1103/PhysRevB.110.125126

I. INTRODUCTION

The topological transition in novel two-dimensional materials with two Dirac cones moving and merging at one point in momentum space has attracted much attention in the literature [1–3]. The corresponding systems are called semi-Dirac systems and support quasiparticles with an effective Hamiltonian that has a relativistic-type linear dispersion along one direction in momentum space and nonrelativistic quadratic dispersion along another direction. Several effective semi-Dirac models were used to describe the physics in black phosphorus [4–9]. In the simplest versions of semi-Dirac models, the additional gap parameter controls whether two bands will be separated, touching at one point, or two Dirac cones will appear [6,7,10–12]. There is a number of experimental realizations of such systems in optical lattices [13] and in microwave cavities [14]. Typically, the parameters of the setup can be tuned to demonstrate different types of quasiparticle spectra in the same system. Many physical properties of semi-Dirac materials have been studied in recent years, including the optical conductivity for different types of semi-Dirac systems [6–9,15,16], the magnetoconductivity [17,18], thermoelectric response [19], Hall conductivity [20], and the unusual scaling of Landau levels with magnetic field [2,3].

In the present paper, we concentrate our attention on the phenomenon of the collapse of Landau levels in an in-plane electric field for the semi-Dirac system. First, the presence of such a phenomenon was discovered for relativistic quasiparticles in graphene [21,22]. It was found that when the electric field strength approaches a certain critical value, the formal solutions for Landau levels become singular. The gap-separated Landau levels are expected to disappear, and a continuous spectrum is formed instead. Such an effect can also be understood in terms of a Lorentz transformation when the effective moving frame speed coincides with the speed of massless quasiparticles [21,23,24]. Later, a Landau level collapse was observed experimentally by measuring the field when Shubnikov–de Haas oscillations disappear for the given sample [25]. Later, it was found that a radial electric field can lead to a similar collapse effect [24].

The Landau level collapse was studied theoretically and experimentally only for systems with a Dirac-type spectrum of quasiparticles. Thus, the general question of the existence of a Landau level collapse in systems with other types of quasiparticle dispersions still needs to be addressed. While the general conclusions for the isotropic dispersion types could be obtained from a semiclassical analysis of the drift velocity, the behavior of Landau level collapse for anisotropic dispersion might contain its own peculiar properties. This motivates our study, and we extended the corresponding part of the Introduction.

There are a number of differences in the collapse of Landau levels that are expected for the semi-Dirac system compared to more typical Dirac semimetals. The main difference is caused by the anisotropic structure of the spectrum, which itself should lead to anisotropy in critical values of the electric field. In addition, a set of two quasiclassically disconnected parts of the Fermi surface is present in the cases of two separated Dirac cones [2,3,7], and one may expect an additional effect of tunneling that will modify the Landau level collapse in such a case. The open question of how a Landau level collapse happens in semi-Dirac models motivates the study in the present paper.

The paper is organized as follows: In Sec. II, we recall the main properties of the low-energy semi-Dirac model with a gap parameter that controls the topological phase transition. Next, in Sec. III, we present semiclassical calculations of Landau levels that appear in crossed electric and magnetic fields. Additionally, we present an asymptotic analysis for the exact Schrödinger equation for such a system. Special attention is given to the case when tunneling (also called magnetic breakdown) takes part and modifies the structure of quasiclassical Landau levels. The corresponding calculations are presented in Sec. IV. Finally, in Sec. V, we compare the results with those known for graphene and give concluding remarks.

II. SEMI-DIRAC MODEL AND TOPOLOGICAL TRANSITION WITH MERGING DIRAC CONES

The effective Hamiltonian that captures separated Dirac cones and the gapped regime as well as the topological transition between them is given by the following expression,

$$H = \left(\Delta + \frac{k_x^2}{2m}\right)\sigma_x + v k_y \sigma_y. \tag{1}$$

There is a number of modifications of this Hamiltonian with higher-order terms or additional gap parameters with another matrix structure [9]. Here, we analyze the simplest version of such a Hamiltonian, which was called "universal" in Refs. [2,3] as it captures the essential physics of the Landau level collapse. The dispersion for each of two bands in the absence of external fields in given by

$$\varepsilon_{\pm}(\boldsymbol{k}) = \pm\sqrt{\left(\frac{k_x^2}{2m} + \Delta\right)^2 + v^2 k_y^2}. \tag{2}$$

The two band-touching Dirac points are separated by the distance $\delta_x = 2\sqrt{2m\Delta}$ in momentum space along the x direction in the case of negative $\Delta < 0$ assuming $m, v > 0$. In the case of zero gap parameter $\Delta = 0$ the two bands touch at $\boldsymbol{k} = 0$.

To include the effects of an electromagnetic field we need to make a Peierls substitution. In the case where the magnetic length is much larger than the spacing of the model, it will result in adding the electrical field term $-e\phi$ and making a transformation $\hat{p} \to \hat{p} + eA$ [26]. This will give us the Hamiltonian

$$H = \left[\Delta + a\left(\hat{p}_x + \frac{e}{c}A_x\right)^2\right]\sigma_x + v\left(\hat{p} + \frac{e}{c}A_y\right)\sigma_y - e\phi. \tag{3}$$

Analyzing the asymptotics in cases $\phi = -Ey$ and $\phi = -Ex$ one can see that when the electrical field is directed along the y axis there always exist bound state solutions, while if it is directed along the x axis all the bound state solutions disappear when

$$\frac{E_x}{B_z} = \frac{v}{c}. \tag{4}$$

However, an attempt to explicitly find the eigenvalues of this Hamiltonian will lead us to a differential equation of the fourth order with many singularities, which is a very nontrivial problem to solve. A semiclassical analysis of this problem has proven to be much more effective.

III. SEMICLASSICAL QUANTIZATION OF CYCLOTRON ORBITS AND MAGNETIC BREAKDOWN

The description of Landau levels in the effective model given by Hamiltonian (1) was presented in Ref. [3]. The main features such as scaling with a magnetic field and a Landau level index can be captured by using the Peierls-Onsager quasiclassical quantization rule, which states that the area of the constant energy curve in momentum space should be quantized,

$$S[\varepsilon(\boldsymbol{k}) = \text{const}] = 2\pi(N + \gamma)eB. \tag{5}$$

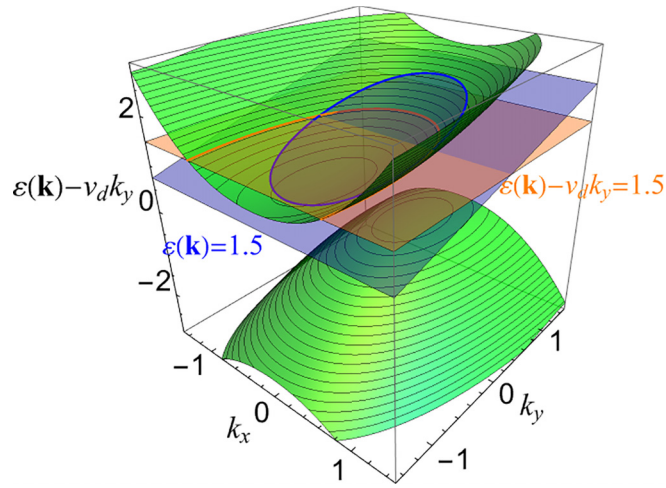

FIG. 1. Spectrum given by Eq. (2) with the additional term $-\boldsymbol{v}_d\boldsymbol{k}$, where $\boldsymbol{v}_d$ is chosen as $(0, -0.5)$. The gap parameter is $\Delta = 1$, and the dispersion parameters are $v = 1$, $a = 1$. As illustrated by the blue plane, when v_d vanishes, the intersection of the plane and the spectrum figure is a closed orbit and thus the Landau level exists. However, as v_d grows, the intersection area increases. As shown at some critical value of v_d the intersection curve becomes an open orbit, as shown with the orange plane, and therefore the collapse of Landau levels is observed.

As was pointed out in Ref. [27], the presence of an electric field modifies the Peierls-Onsager quantization rule,

$$S[\varepsilon(\boldsymbol{k}) - \boldsymbol{v}_d\boldsymbol{k} = \text{const}] = 2\pi(N + \gamma)eB, \tag{6}$$

with the classical drift velocity in crossed fields defined as $\boldsymbol{v}_d = c\boldsymbol{E} \times \boldsymbol{B}/\boldsymbol{B}^2$. Here, the "const" on the left-hand side of the dispersion equation takes into account that the contour in k space contains all the points for which the value of the expression $\varepsilon(\boldsymbol{k}) - \boldsymbol{v}_d\boldsymbol{k}$ is fixed. Different Landau level indices N would eventually result in different values of const. Before proceeding with more detailed calculations, let us perform a qualitative analysis. The collapse of Landau levels is associated with the fact that the area defined by a contour in momentum space $\varepsilon(\boldsymbol{k}) - \boldsymbol{v}_d\boldsymbol{k} = \text{const}$ becomes infinite. This may happen either for a Landau level with a particular index or for all levels simultaneously. Consequently, the general criteria for the presence of a Landau level collapse for the band spectrum in infinite momentum space $-\infty < k_{x,y} < \infty$ is equivalent to the question of the absence of closed curves of solutions for the equation $\varepsilon(\boldsymbol{k}) - \boldsymbol{v}_d\boldsymbol{k} = \text{const}$ with a fixed right-hand side constant. The geometrical interpretation of this criterion can be formulated in terms of the shape of intersection curves of the dispersion $\varepsilon(\boldsymbol{k})$ and the plane $\boldsymbol{v}_d\boldsymbol{k} + \text{const} = 0$, as illustrated in Fig. 1. Such an intersection becomes an open curve when the dispersion grows slower than linear with a prefactor $\boldsymbol{v}_d$ at large momenta values:

$$\varepsilon(\boldsymbol{k} \to \infty) \lesssim \boldsymbol{v}_d\boldsymbol{k}. \tag{7}$$

This formula allows one to predict the existence of a Landau level collapse by analyzing the asymptotic behavior of dispersion.

Applying (7) to the dispersion of the semi-Dirac model and taking asymptotics along two orthogonal directions,

$$\varepsilon_+(k_x \to \infty) \sim \frac{k_x^2}{2m}, \quad \varepsilon_\pm(k_y \to \infty) \sim \pm v k_y, \tag{8}$$

we find that the collapse of the Landau levels is possible for the case of drift velocity having a nonzero component along the y direction. The collapse occurs for all energy levels simultaneously when this component is greater than the parameter of the model $v_{d,y} > v$. For the case of a uniform constant electric and magnetic field with the B field along the z direction, this leads to the fact that the electric field should have a nonzero component along the x direction, with a critical value for the collapse:

$$E_x = v B_z / c. \tag{9}$$

For the electric field directed along the y axis of the model, the collapse of Landau levels is not possible. One can see that this is exactly the result (4) that we got by analyzing the asymptotics. However, semiclassics allows for a more detailed study of energy levels.

IV. ENERGY LEVELS IN THE PRESENCE OF AN ELECTROMAGNETIC FIELD

To calculate energy levels we will use Eq. (6). Full technical calculations are given in the Appendix, but the main idea is to notice that the resulting closed orbit could be described by the equation

$$\left(\frac{k_x^2}{2m} + \Delta\right)^2 + \left(v^2 - v_d^2\right)\left(k_y - \frac{v_d \varepsilon^*(\boldsymbol{k})}{v^2 - v_d^2}\right)^2 = \frac{v^2}{v^2 - v_d^2}\varepsilon^{*2}, \tag{10}$$

where $\varepsilon^*(\boldsymbol{k}) = \varepsilon(\boldsymbol{k}) - \boldsymbol{v}_d \boldsymbol{k}$. Denoting $\tilde{E} = \frac{v}{\sqrt{v^2 - v_d^2}}\varepsilon^*$ and $\tilde{k}_y = (k_y - \frac{v_d \varepsilon^*(\boldsymbol{k})}{v^2 - v_d^2})$ we can express the area of the orbit as

$$S(k_x, k_y) = \iint dk_x d\tilde{k}_y \theta\left[\tilde{E}^2 - \left(\frac{k_x^2}{2m} + \Delta\right)^2 - \left(v^2 - v_d^2\right)\tilde{k}_y^2\right]. \tag{11}$$

In the case of $\Delta \geqslant 0$ the equation for energy levels has the form

$$\frac{\pi(|\tilde{E}| - \Delta)\sqrt{|\tilde{E}| + \Delta}}{4\sqrt{a}\sqrt{v^2 - v_d^2}} F\left(\frac{1}{2}, \frac{3}{2}, 3, -\frac{|\tilde{E}| - \Delta}{|\tilde{E}| + \Delta}\right) = 2\pi(N + \gamma)\frac{eB}{c}. \tag{12}$$

This equation can be solved numerically. In Fig. 2 we plot the solution for a particular Δ, but the whole form is quite general for the case $\Delta \geqslant 0$.

In the case of negative gap parameter $\Delta < 0$ the effective dispersion (2) contains two Dirac points separated in momentum space. As a result, there are two possible closed "orbits" (see Fig. 3).

In this situation there is a possibility of tunneling between two orbits which influences the energy level structure. The tunneling probability decays exponentially with the energy

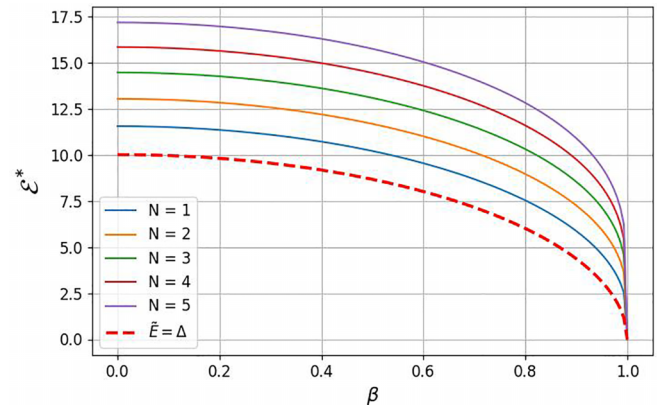

FIG. 2. Numerical solution for Eq. (12) with "+" in Eq. (2) and $\Delta = mv^2 = \frac{eB}{mc}$. Energy levels are labeled with N. Here, $\beta = \frac{v_d}{v}$ and ε^* is measured in units of $\frac{eB}{mc}$. As β reaches 1, the energy levels collapse.

deviation from the saddle point level. Thus, we should implement a double-well representation to properly describe the semiclassical spectrum around that point. The complete theory of the corresponding semiclassical description was presented in Ref. [28]. Here, we use the quantization condition derived from this description,

$$\cos\left[\frac{\Omega_1 + \Omega_2}{2} + \phi(\mu)\right] = |\mathcal{T}(\mu)| \cos\left[\frac{\Omega_1 - \Omega_2}{2}\right], \tag{13}$$

where $\Omega_j = \pi + \frac{eB}{c}S_j + \int_0^1 \frac{\tilde{H}_1^{v(t_j)}}{v_{v(t_j)}^x}\frac{dk}{dt_j}dt_j + (-1)^{j+1}\delta_y^B$. Here, S_j is the area of the corresponding orbit, $\mathcal{T}(\mu)$ is the scattering matrix in the Peierls-Onsager approximation, $\tilde{H}_1 = H_1^R + H_1^Z + H_1^B - H_1(0)$ correspond to Roth, Zeeman, and Berry corrections, and δ_y^B is an additional Berry phase. Since in our case Berry curvature is equal to zero and the Zeeman Hamiltonian is absent, the only term left is the area of the orbit in k space S_j. Noticing that the areas of the orbits are identical,

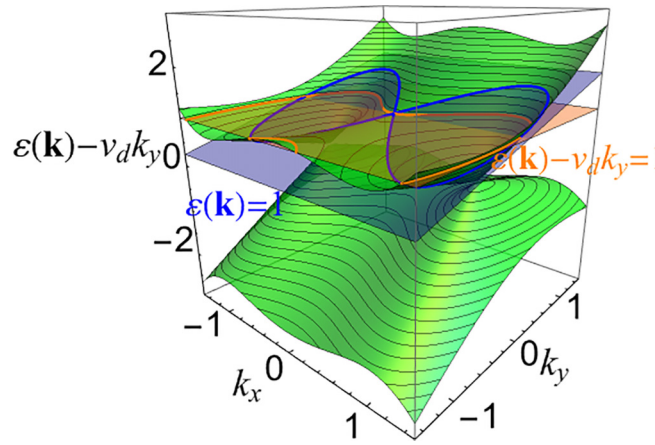

FIG. 3. The same as in Fig. 1, but for $\Delta = -1$. Note that depending on the energy either one or two independent closed figures can emerge.

we get the expression

$$\cos\left[\frac{c}{eB}S+\phi(\mu)\right]=-\frac{e^{\pi\mu/2}}{\sqrt{2\cosh\pi\mu}}. \tag{14}$$

The area of an orbit can be calculated by the same method we used earlier. Denoting $\delta=|\frac{\tilde{E}}{\Delta}|$ and using Eq. (11) we obtain

$$S=\frac{\sqrt{2m}|\Delta|^{\frac{3}{2}}\delta^2\sqrt{1-\delta}}{2\sqrt{v^2-v_d^2}}F\left(\frac{1}{2},\frac{3}{2},3,-\frac{2\delta}{1-\delta}\right). \tag{15}$$

Using the definitions of ϕ and μ from Ref. [28],

$$\phi(\mu)=\arg\left[\Gamma\left(\frac{1}{2}-i\mu\right)\right]+\mu[\ln(|\mu|)-1], \tag{16}$$

$$\mu=\pm\sqrt{\frac{2m}{v^2-v_d^2}}\frac{c|\Delta|^{\frac{3}{2}}}{eB}(1-\delta), \tag{17}$$

where $\mp$ corresponds to the branch choice in Eq. (2). Solving this final equation numerically, we get the structure of energy levels described in Fig. 4.

One can notice that the conditions for the collapse of Landau levels do not depend on Δ and happen when $\beta=1$.

One can observe a peculiar effect: the birth of pairs of energy levels with an increase of the electrical field. The mathematical origin of such a solution can be illustrated fairly straightforwardly.

Let us take the limit $\mu\gg1$ in Eq. (14), which arises at relatively small energies and large fields. In this limit, we can use the form of Stirling's approximation for complex arguments with a large absolute value (see Chap. IV in Ref. [29]) and expand $\arg[\Gamma(\frac{1}{2}-i\mu)]\approx-\mu(\ln\mu-1)$. Then, Eq. (14) turns into

$$\cos\left[\frac{c\sqrt{2m}|\Delta|^{\frac{3}{2}}}{2eB\sqrt{v^2-v_d^2}}\delta^2\sqrt{1-\delta}F\left(\frac{1}{2},\frac{3}{2},3,-\frac{2\delta}{1-\delta}\right)\right]=-1. \tag{18}$$

Denoting $\frac{c\sqrt{2m}|\Delta|^{\frac{3}{2}}}{2eB\sqrt{v^2-v_d^2}}$ as $\tilde{\omega}$ we can rewrite the equation as

$$\cos\left[\tilde{\omega}\delta^2\sqrt{1-\delta}F\left(\frac{1}{2},\frac{3}{2},3,-\frac{2\delta}{1-\delta}\right)\right]=-1. \tag{19}$$

Now, let us denote the function

$$f(\delta)=\delta^2\sqrt{1-\delta}F\left(\frac{1}{2},\frac{3}{2},3,-\frac{2\delta}{1-\delta}\right) \tag{20}$$

and look at this function at the point $\delta=\delta_0$, such that $\frac{d}{d\delta}f(\delta)=0|_{\delta=\delta_0}$. Figure 5 suggests that there is only one point like that. This point is also an extremum for the function $\cos[\tilde{\omega}f(\delta)]$. Moreover, this is an extremum of that function for any $\tilde{\omega}$. We can see that because the function $f(\delta)$ is continuously growing on the interval $(0,\delta_0)$ and is continuously decaying on the $(\delta_0,1)$, different $\tilde{\omega}$ just correspond to different oscillation frequencies and thus there are two different times the cos function touches the line $f(\delta)=-1$. The new pair of levels is born whenever $\cos[\tilde{\omega}f(\delta_0)]=-1$. From here we can write the condition on the birth of a pair of levels as

$$\sqrt{1-\beta_*^2}=\frac{c\sqrt{2m}|\Delta|^{\frac{3}{2}}}{2eBv}\frac{f(\delta_0)}{\pi+2\pi n}, \tag{21}$$

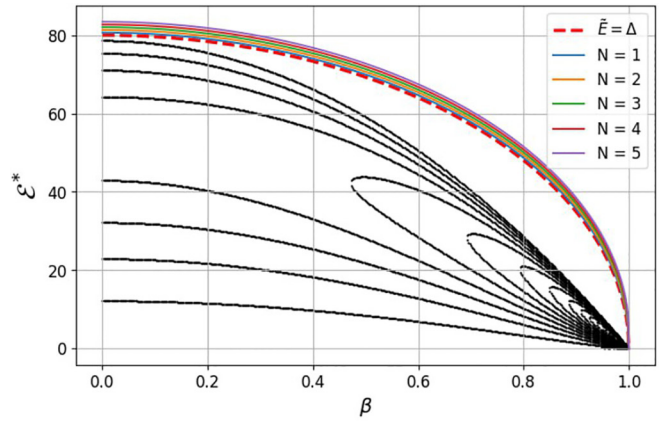

(a) $\Delta=-\frac{1}{4}\frac{eB}{mc}$

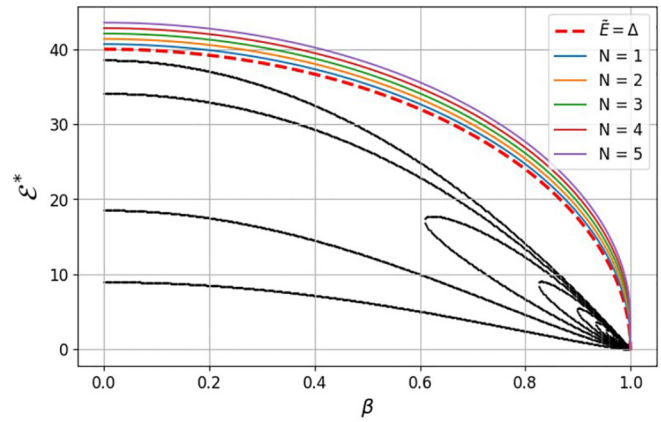

(b) $\Delta=-\frac{1}{2}\frac{eB}{mc}$

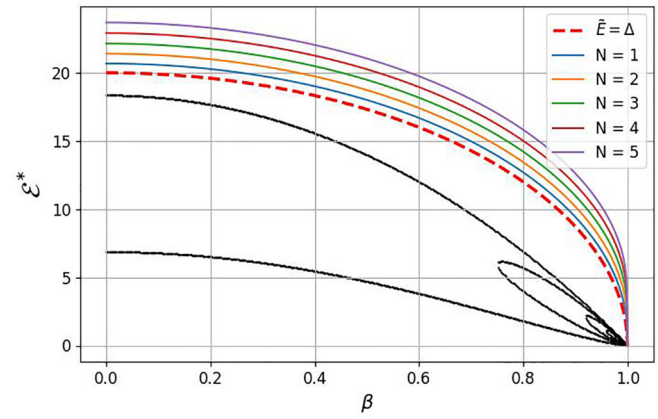

(c) $\Delta=-\frac{eB}{mc}$

FIG. 4. Numerical solution for Eq. (14) with "+" in Eq. (2). High-energy levels (labeled with N) have the same structure as in Fig. 2. The energy levels below $\tilde{E}=|\Delta|$ (shown with black lines) possess a different structure, including the emergence of "loops." As before, $\beta=\frac{v_d}{v}$, $\Delta=-2mv^2$, and ε^* is measured in units of $\frac{eB}{mc}$. The magnetic field is increased two times from picture to picture. The stronger the magnetic field, the fewer levels are below the saddle point $\mathcal{E}=\Delta$. (a) $\Delta=-\frac{1}{4}\frac{eB}{mc}$, (b) $\Delta=-\frac{1}{2}\frac{eB}{mc}$, (c) $\Delta=-\frac{eB}{mc}$.

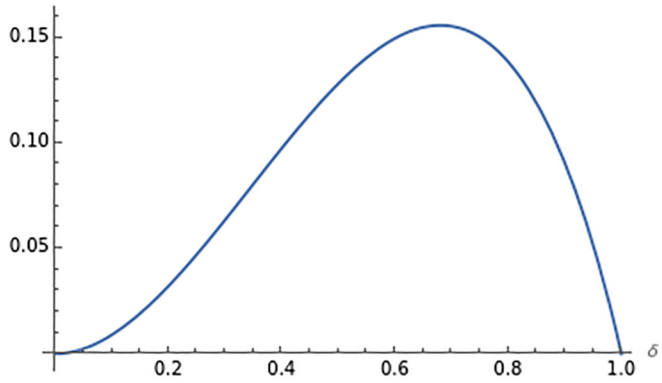

FIG. 5. Plot of the function $f(\delta)$ defined in Eq. (20).

where β_* are the values of $\frac{v_d}{v}$ at which new pairs of levels are born. The numerical calculations show that $f(\delta_0) = 0.155\,829$. The observed appearance of pairs of energy levels with growing electric field can be understood in the following way: This phenomenon happens on the level of a saddle point, where the tunneling effects are strong. For a typical Landau level the orbit remains closed with changing electric field, thus the Landau level energy moves to a lower energy. In the case of Landau levels near the saddle point the orbit might pass the saddle point level and break down. Such a modified quantization rule might allow for the appearance of new allowed Landau levels when the effective dispersion $\mathcal{E}^*$ deforms under a growing electric field.

V. CONCLUSIONS

To summarize, we have analyzed the semi-Dirac model subjected to in-plane electric and out-of-plane magnetic fields and found the condition for the appearance of the Landau level collapse phenomenon. Based on a semiclassical WKB-type approach, we found that the Landau level collapse appears only when the effective dispersion grows as a linear function of momentum or slower. Application of these general criteria as well as an exact derivation of semiclassical Landau level (LL) dispersion from the constant energy curves modified by an electric field have shown that the LL collapse happens only for one direction of electric field. In other words, only an electric field with the x component exceeding the threshold leads to LL collapse. This result can be contrasted with the example of monolayer graphene, where any direction of the electric field has the possibility to make a collapse.

In addition, we analyzed the structure of LL for electric field values close to collapse for the gap parameter of the model corresponding to three topologically distinct cases (two Dirac cones, one band touching point, and two gapped bands). We have discovered that in the case of the negative gap parameter $\Delta < 0$ the number of Landau levels below the saddle point increases.

ACKNOWLEDGMENTS

We would like to express our gratitude to Leonid Levitov and Dmytro Oriekhov for the idea of the project and for their guidance and help. We would also like to thank Yelizaveta Kulynych for helpful discussions.

APPENDIX: EVALUATION OF AREA INTEGRALS FOR SEMICLASSICAL QUANTIZATION

The effective dispersion of the semi-Dirac model has the form

$$\varepsilon(\boldsymbol{k}) = \pm\sqrt{\left(\frac{k_x^2}{2m} + \Delta\right)^2 + v^2 k_y^2}. \tag{A1}$$

It predicts the relativistic dispersion along one direction and nonrelativistic along another (and a mix in between). The "unusual" power law comes from the anisotropy of the model and the corresponding constant energy curve area function with energy. The Landau level collapse happens when the electrical field has the component $E_x > \frac{v}{c}H$. The E_y component has no effect on the collapse.

Let us find semiclassical energy levels in the presence of an electrical field. The modified dispersion [27]

$$\varepsilon^*(\boldsymbol{k}) = \pm\sqrt{\left(\frac{k_x^2}{2m} + \Delta\right)^2 + v^2 k_y^2} - v_d k_y = \text{const}\,. \tag{A2}$$

In order to find areas in the momentum space it is convenient to rewrite this equation as

$$\left(\frac{k_x^2}{2m} + \Delta\right)^2 + \left(v^2 - v_d^2\right)\left(k_y - \frac{v_d \varepsilon^*(\boldsymbol{k})}{v^2 - v_d^2}\right)^2 = \frac{v^2}{v^2 - v_d^2}\varepsilon^{*2}. \tag{A3}$$

From this equation it is clear the electrical field corresponds only to the scaling of energy levels, and does not lead to other significant effects. It is worth noting that here we can see the collapse arising at $v_d = v$.

Let us denote in the following calculations that $\frac{v^2}{v^2 - v_d^2}\varepsilon^{*2} = \tilde{E}^2$ and $(k_y - \frac{v_d \varepsilon^*(\boldsymbol{k})}{v^2 - v_d^2}) = \tilde{k}_y$. The area of orbit in the momentum space can be calculated as

$$S(k_x, k_y) = \iint dk_x d\tilde{k}_y \theta\left[\tilde{E}^2 - \left(\frac{k_x^2}{2m} + \Delta\right)^2 - \left(v^2 - v_d^2\right)\tilde{k}_y^2\right]. \tag{A4}$$

There are two cases we need to study: $\Delta \geqslant 0$ and $\Delta < 0$. Let us start with the first case. The integral comes down to

$$S(k_x, k_y) = \frac{2}{\sqrt{v^2 - v_d^2}} \int_{-\sqrt{2m}\sqrt{|\tilde{E}| - \Delta}}^{\sqrt{2m}\sqrt{|\tilde{E}| - \Delta}} \sqrt{\tilde{E}^2 - \left(\frac{k_x^2}{2m} + \Delta\right)^2}\, dk_x, \tag{A5}$$

and can be transformed to

$$S(k_x, k_y) = \frac{2\sqrt{2m}(|\tilde{E}| - \Delta)^{\frac{3}{2}}}{\sqrt{v^2 - v_d^2}} \times \int_{-1}^{1} \sqrt{\frac{\tilde{E}^2}{(|\tilde{E}| - \Delta)^2} - \left(x^2 + \frac{|\tilde{E}|}{(|\tilde{E}| - \Delta)} - 1\right)^2}\, d. \tag{A6}$$

From here, changing the integration variable to $d(x^2)$ and using the integral representation of the hypergeometric function

$$F(a,b,c,z) = \frac{\Gamma(c)}{\Gamma(b)\Gamma(c-b)} \times \int_0^1 t^{b-1}(1-t)^{c-b-1}(1-zt)^{-a}\,dt, \quad \text{(A7)}$$

we get that

$$S(k_x,k_y) = \frac{2\sqrt{2m}(|\tilde{E}|-\Delta)\sqrt{|\tilde{E}|+\Delta}}{\sqrt{v^2-v_d^2}} \times F\left(\frac{1}{2},\frac{3}{2},3,-\frac{|\tilde{E}|-\Delta}{|\tilde{E}|+\Delta}\right) = 2\pi\frac{eB}{c}(n+\gamma). \quad \text{(A8)}$$

When $\Delta < 0$ an interband breakdown for some energy levels can arise, so our quantization rule should be modified. When $|\frac{\tilde{E}}{\Delta}| = \delta \geqslant 1$, formula (A8) holds for negative Δ as well. However, when $\delta < 1$ there exist two closed classical orbits and there is a possibility of tunneling between them. This case is described in Ref. [28]:

$$\cos\left[\frac{\Omega_1+\Omega_2}{2}+\phi(\mu)\right] = |\mathcal{T}(\mu)|\cos\left[\frac{\Omega_1-\Omega_2}{2}\right]. \quad \text{(A9)}$$

In our case, with the absence of Berry's curvature and the Zeeman Hamiltonian, Ω_1 and Ω_2 are just equal to the dimensionless surfaces of both trajectories in the momentum space. As we can see from Eq. (A4) the surfaces are equal to each other. Using Eq. (A4) we obtain four possible "stop points"—the integration limits for surface calculation: $k_x = \pm\sqrt{2m(|\Delta| \pm |\tilde{E}|)}$. Transforming to dimensionless variables we get

$$S_1 = S_2 = \frac{2\sqrt{2m}|\Delta|^{\frac{3}{2}}}{\sqrt{v^2-v_d^2}}\int_{-\sqrt{1-\delta}}^{-\sqrt{1+\delta}}\sqrt{\delta^2-(x^2-1)^2}\,dx. \quad \text{(A10)}$$

Changing the integration variable to $\frac{x^2-1}{\delta}$ and expanding the expression as $(\delta+1-x^2)(\delta+x^2-1)$ we will get

$$S = \frac{2\sqrt{2m}|\Delta|^{\frac{3}{2}}\delta^2}{\sqrt{v^2-v_d^2}}\int_{-1}^{1}\sqrt{(1-x)(1+x)}(1+\delta x)\,dx. \quad \text{(A11)}$$

From here it is easy to obtain the integral representation of a hypergeometric function (A7) by changing the integration variable to $\frac{1+x}{2}$ and as a result we get

$$S = \frac{\sqrt{2m}|\Delta|^{\frac{3}{2}}\delta^2\sqrt{1-\delta}}{2\sqrt{v^2-v_d^2}}F\left(\frac{1}{2},\frac{3}{2},3,-\frac{2\delta}{1-\delta}\right). \quad \text{(A12)}$$

We take μ, $\phi(\mu)$, and $\mathcal{T}(\mu)$ as defined in Ref. [28],

$$\mu = \pm\sqrt{\frac{2m}{v^2-v_d^2}}\frac{c|\Delta|^{\frac{3}{2}}}{eB}(1-\delta), \quad \text{(A13)}$$

where the choice of the sign corresponds to the branch choice in Eq. (A2) [note that Eq. (A12) includes both branches due to the modulus of $\tilde{E}$]. So,

$$\phi(\mu) = \arg\left[\Gamma\left(\frac{1}{2}-i\mu\right)\right] + \mu[\ln(|\mu|)-1], \quad \text{(A14)}$$

$$\mathcal{T}(\mu) = e^{i\phi(\mu)}\frac{e^{\pi\mu/2}}{\sqrt{2\cosh\pi\mu}}, \quad \text{(A15)}$$

and all that is left to do is to put them into this final equation,

$$\cos\left[\frac{c}{eB}S+\phi(\mu)\right] = -\frac{e^{\pi\mu/2}}{\sqrt{2\cosh\pi\mu}}. \quad \text{(A16)}$$

An approximate solution of this equation could be found with the right estimation for $\arg[\Gamma(\frac{1}{2}-i\mu)]$. To find this estimation, we use the Weierstrass's definition of the Γ function

$$\Gamma(z) = \frac{e^{-\gamma z}}{z}\prod_{n=1}^{\infty}\left(1+\frac{z}{n}\right)^{-1}e^{z/n}, \quad \text{(A17)}$$

where γ is the Euler-Mascheroni constant.

Let us define the phase ϕ_n as $(z+n) = |z+n|e^{i\phi_n}$. Then, according to (A17),

$$\arg\left[\Gamma\left(\frac{1}{2}-i\mu\right)\right] = \gamma\mu - \phi_0 - \sum_{n=1}^{\infty}\left(\frac{\mu}{n}+\phi_n\right), \quad \text{(A18)}$$

where we can take $\phi_n = -\arcsin(\frac{\mu}{\sqrt{(n+\frac{1}{2})^2+\mu^2}})$. Using the approximation $\sum_{n=1}^{\infty}f(n) \approx \int_1^{\infty}f(x)dx$ for slowly changing functions (which applies to $\frac{1}{x}$ when $x \geqslant 1$) we get

$$\arg\left[\Gamma\left(\frac{1}{2}-i\mu\right)\right] \approx \gamma\mu + \arcsin\frac{\mu}{\sqrt{\frac{1}{4}+\mu^2}} \times + \int_1^{\infty}\left(\arcsin\frac{\mu}{\sqrt{\left(x+\frac{1}{2}\right)^2+\mu^2}} - \frac{\mu}{x}\right)dx. \quad \text{(A19)}$$

Expanding $\arcsin(\frac{\mu}{\sqrt{(x+\frac{1}{2})^2+\mu^2}}) = x'\arcsin(\frac{\mu}{\sqrt{(x+\frac{1}{2})^2+\mu^2}})$ we get

$$\int \arcsin\left(\frac{\mu}{\sqrt{\left(x+\frac{1}{2}\right)^2+\mu^2}}\right)dx = x\arcsin\left(\frac{\mu}{\sqrt{\left(x+\frac{1}{2}\right)^2+\mu^2}}\right) + \frac{\mu}{2}\ln\left[\mu^2+\left(x+\frac{1}{2}\right)^2\right]+C,$$

and therefore

$$\arg\left[\Gamma\left(\frac{1}{2}-i\mu\right)\right] \approx \gamma\mu+\mu-\frac{\mu}{2}\ln\left(\mu^2+\frac{9}{4}\right) + \arcsin\frac{\mu}{\sqrt{\frac{1}{4}+\mu^2}} - \arcsin\frac{\mu}{\sqrt{\frac{9}{4}+\mu^2}}. \quad \text{(A20)}$$

Now, let us look at two asymptotics $|\mu| \gg 1$ and $|\mu| \ll 1$. Expanding (A20) for both cases we get

$$\phi(\mu) \approx \gamma\mu, \text{ when } |\mu| \gg 1,$$
$$\phi(\mu) \approx \left(\gamma + \ln\frac{3}{2}\right)\mu + \mu \ln|\mu|, \text{ when } |\mu| \ll 1. \tag{A21}$$

Equation (A16) turns into

$$\cos\left(\frac{c}{eB}S + \gamma\mu\right) \approx 1, \text{ when } |\mu| \gg 1,$$
$$\cos\left[\frac{c}{eB}S + \left(\gamma + \ln\frac{3}{2}\right)\mu + \mu\ln|\mu|\right] \approx \frac{1}{\sqrt{2}} - \frac{\pi}{2}\mu, \text{ when } |\mu| \ll 1. \tag{A22}$$

[1] Y. Hasegawa, R. Konno, H. Nakano, and M. Kohmoto, Zero modes of tight-binding electrons on the honeycomb lattice, Phys. Rev. B **74**, 033413 (2006).

[2] G. Montambaux, F. Piéchon, J.-N. Fuchs, and M. O. Goerbig, Merging of Dirac points in a two-dimensional crystal, Phys. Rev. B **80**, 153412 (2009).

[3] G. Montambaux, F. Piéchon, J.-N. Fuchs, and M. O. Goerbig, A universal Hamiltonian for motion and merging of Dirac points in a two-dimensional crystal, Eur. Phys. J. B **72**, 509 (2009).

[4] M. Ezawa, Highly anisotropic physics in phosphorene, J. Phys.: Conf. Ser. **603**, 012006 (2015).

[5] P. K. Pyatkovskiy and T. Chakraborty, Dynamical polarization and plasmons in a two-dimensional system with merging Dirac points, Phys. Rev. B **93**, 085145 (2016).

[6] J. P. Carbotte, K. R. Bryenton, and E. J. Nicol, Optical properties of a semi-Dirac material, Phys. Rev. B **99**, 115406 (2019).

[7] J. P. Carbotte and E. J. Nicol, Signatures of merging Dirac points in optics and transport, Phys. Rev. B **100**, 035441 (2019).

[8] P. Adroguer, D. Carpentier, G. Montambaux, and E. Orignac, Diffusion of Dirac fermions across a topological merging transition in two dimensions, Phys. Rev. B **93**, 125113 (2016).

[9] J. Jang, S. Ahn, and H. Min, Optical conductivity of black phosphorus with a tunable electronic structure, 2D Mater. **6**, 025029 (2019).

[10] E. Illes, J. P. Carbotte, and E. J. Nicol, Hall quantization and optical conductivity evolution with variable Berry phase in the α-T_3 model, Phys. Rev. B **92**, 245410 (2015).

[11] E. Illes and E. J. Nicol, Magnetic properties of the α-T_3 model: Magneto-optical conductivity and the Hofstadter butterfly, Phys. Rev. B **94**, 125435 (2016).

[12] D. O. Oriekhov and V. P. Gusynin, Optical conductivity of semi-Dirac and pseudospin-1 models: Zitterbewegung approach, Phys. Rev. B **106**, 115143 (2022).

[13] L. Tarruell, D. Greif, T. Uehlinger, G. Jotzu, and T. Esslinger, Creating, moving and merging Dirac points with a Fermi gas in a tunable honeycomb lattice, Nature (London) **483**, 302 (2012).

[14] M. Bellec, U. Kuhl, G. Montambaux, and F. Mortessagne, Topological transition of Dirac points in a microwave experiment, Phys. Rev. Lett. **110**, 033902 (2013).

[15] K. Ziegler and A. Sinner, Lattice symmetries, spectral topology and opto-electronic properties of graphene-like materials, Europhys. Lett. **119**, 27001 (2017).

[16] A. Mawrie and B. Muralidharan, Direction-dependent giant optical conductivity in two-dimensional semi-Dirac materials, Phys. Rev. B **99**, 075415 (2019).

[17] X. Zhou, W. Chen, and X. Zhu, Anisotropic magneto-optical absorption and linear dichroism in two-dimensional semi-Dirac electron systems, Phys. Rev. B **104**, 235403 (2021).

[18] P. Sinha, S. Murakami, and S. Basu, Landau levels and magneto-optical transport properties of a semi-Dirac system, Phys. Rev. B **105**, 205407 (2022).

[19] I. Mandal and K. Saha, Thermoelectric response in nodal-point semimetals, Ann. Phys. **536**, 2400016 (2024).

[20] P. Sinha, S. Murakami, and S. Basu, Quantum Hall studies of a semi-Dirac nanoribbon, Phys. Rev. B **102**, 085416 (2020).

[21] V. Lukose, R. Shankar, and G. Baskaran, Novel electric field effects on Landau levels in graphene, Phys. Rev. Lett. **98**, 116802 (2007).

[22] N. M. R. Peres and E. V. Castro, Algebraic solution of a graphene layer in transverse electric and perpendicular magnetic fields, J. Phys.: Condens. Matter **19**, 406231 (2007).

[23] A. Shytov, M. Rudner, N. Gu, M. Katsnelson, and L. Levitov, Atomic collapse, Lorentz boosts, Klein scattering, and other quantum-relativistic phenomena in graphene, Solid State Commun. **149**, 1087 (2009).

[24] I. O. Nimyi, V. Könye, S. G. Sharapov, and V. P. Gusynin, Landau level collapse in graphene in the presence of in-plane radial electric and perpendicular magnetic fields, Phys. Rev. B **106**, 085401 (2022).

[25] N. Gu, M. Rudner, A. Young, P. Kim, and L. Levitov, Collapse of Landau levels in gated graphene structures, Phys. Rev. Lett. **106**, 066601 (2011).

[26] M. O. Goerbig, Electronic properties of graphene in a strong magnetic field, Rev. Mod. Phys. **83**, 1193 (2011).

[27] I. M. Lifshitz and M. I. Kaganov, Some problems of the electron theory of metals I. Classical and quantum mechanics of electrons in metals, Sov. Phys. Usp. **2**, 831 (1960).

[28] A. Alexandradinata and L. Glazman, Semiclassical theory of Landau levels and magnetic breakdown in topological metals, Phys. Rev. B **97**, 144422 (2018).

[29] E. C. Titchmarsh, *The Theory of the Riemann Zeta-Function* (Oxford Science, Oxford, UK, 1987).